Ultrafast Electron Transfer in Photosynthesis: Reduced Pheophytin and Quinone Interaction Mediated by Conical Intersections

Gloria Olaso-González, Manuela Merchán, and Luis Serrano-Andrés*

Instituto de Ciencia Molecular, Universitat de València, Apartado 22085, ES-46071 Valencia, Spain

Received: June 22, 2006; In Final Form: September 20, 2006

The mechanism of electron transfer (ET) from reduced pheophytin ($Pheo^-$) to the primary stable photosynthetic acceptor, a quinone (Q) molecule, is addressed by using high-level ab initio computations and realistic molecular models. The results reveal that the ET process involving the ($Pheo^- + Q$) and ($Pheo + Q^-$) oxidation states can be essentially seen as an ultrafast radiationless transition between the two hypersurfaces taking place via conical intersections (CIs). According to the present findings, an efficient ultrafast ET implies that the $Pheo^-$ and Q move toward each other in a given preferential parallel orientation, reaching the most effective arrangement for ET at intermolecular distances (R) around 5−3 Å, where the lowest CIs are predicted. Favored donor/acceptor interactions are related to orientations with some overlap between the lowest occupied molecular orbitals (LUMO) of the two systems, and they lead to state-crossings at an earlier stage of the movement (larger R). Furthermore, when the topology of the interacting moieties does not make possible the LUMOs overlap, the corresponding diabatic potential energy curves do not intersect. Thus, it is anticipated that large scale motions, which are difficult to monitor experimentally, are actually occurring in the photosynthetic reaction centers of bacteria, algae, and higher plants, to fulfill the observed ultrafast ET processes.

1. Introduction

A vast amount of information about photosynthesis is currently available thanks to the efforts of numerous researchers along the past two centuries and it keeps growing considerably every day.[1−8] Nevertheless, to achieve a detailed knowledge of the entire process of transformation of solar into chemical energy in the photosynthetic reaction centers (RCs) of bacteria, algae, and higher plants still represents a true challenge, from both experimental and theoretical standpoints. It is clear that learning about photosynthesis means a better understanding of life on earth as we know and it is also well recognized that the realm of photosynthesis has become truly interdisciplinary. Apart from its intrinsic interest, research in the field is essential in synthetic organic chemistry, nanotechnology, and material science, whereas bioinspired devices have been successfully designed and their performance is increasing continuously.[9] Because of the outstanding development of computational methods and tools, the discipline of quantum chemistry may help to unravel, and it indeed does,[10−18] certain aspects of the extraordinarily complex mechanisms involved in the RCs that can hardly be deduced from direct experiments.

The purple bacteria RC is probably the most studied and best understood photosynthetic system.[1,8,15] Upon excitation of the special pair (SP) dimer of bacteriochlorophyll (BChl) *a* molecules (more frequently found than BChl *b*), charge separation occurs within a few picoseconds, yielding the oxidized special pair (SP^+) and a reduced bacteriopheophytin ($BPheo^-$). The captured electron is subsequently transferred to ubiquinone in about 200 ps.[4] In oxygenic photosynthesis a simultaneous excitation of pairs of chlorophyll (Chl) *a* molecules, labeled as P680 in photosystem II (PSII) and P700 in photosystem I (PSI), also takes place, producing oxidized P680 ($P680^+$) and reduced Pheo ($Pheo^-$) in PSII. Pheo is a pheophytin molecule that can be viewed as a chlorophyll moiety with the central magnesium ion replaced by two hydrogen atoms (see Figure 1) and it is the actual primary electron acceptor of PSII. The extra electron of $Pheo^-$ is then rapidly given to the plastoquinone molecule, considered as the primary *stable* electron acceptor of PSII. Therefore, both bacteria and plants proceed through a similar scheme. Once the photoinduced charge separation on excited RCs occurs, a quinone-like system is capable of gaining the electron localized on a reduced pheophytin-like molecule in a time regime of picoseconds. What is the underlying mechanism of this ultrafast electron transfer (ET)? Answering to this question has been the main motivation to undertake the present research.

Understanding the mechanism involved in ET reactions is both intriguing and challenging.[19] Nowadays, it constitutes one of the most active areas of research in physical chemistry. It is well-known that ET processes are encountered quite often in biological functions in connection with the transduction of energy that ultimately leads to a biochemical signal. They are usually described within the framework of quasi-equilibrium schemes, Marcus' theory being the most popular.[20] In photosynthesis, ETs have two specific characteristics: (i) they are activationless, that is, they take place in the so-called inverted region of the Marcus theory, and (ii) they proceed very fast and in the same order of magnitude as the time scale of vibrational motion (in the femto- or picosecond regime) and consequently nonequilibrium aspects cannot be discarded. In this sense, ultrafast ET reactions can essentially be seen as radiationless transitions of the supersystem because of the breakdown of quasi-equilibrium dynamic models.[17,19] The relationship between the Marcus−Hush diagrams and the topology of the conical intersections for different intramolecular electron transfer rearrangements has been discussed in detail by Blancafort et al.[21] A large body of experimental and

* To whom correspondence should be addressed. E-mail: Luis.Serrano@uv.es.

10.1021/jp063915u CCC: $33.50
Published on Web 11/14/2006

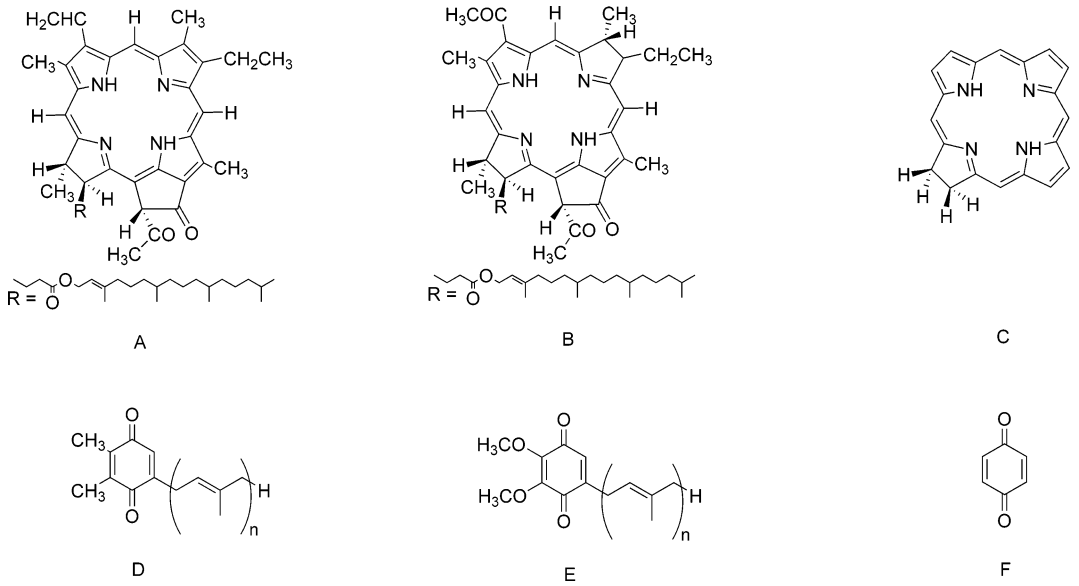

Figure 1. Structures of pheophytin *a* (A), bacteriopheophytin *a* (B), chlorin (C), plastoquinone (D), ubiquinone (E), and *p*-benzoquinone (F).

theoretical work involving a complete variety of relevant biological chromophores, including electron-transfer reactions, supports today that efficient ultrafast nonradiative transitions are mediated by conical intersections (CIs).[22−26] True electronic degeneracy occurs at a CI point, which is lifted in at least two directions, which are functions of nuclear coordinates. The denomination *conical intersection* comes from the fact that the corresponding hypersurfaces at a CI point have the shape of a double cone when the energy of the upper and lower state is plotted against those privileged coordinates. An infinite number of CI points form a crossing seam or hyperline between two states of the same multiplicity. To describe the dynamics of photochemical reactions, full characterization of the hyperline is essential. Normally, in practice, efficient transition from one state to the other is expected to take place mainly around the region of the lowest energy point of the hyperline, i.e., at the lowest CI.[22] Thus, most of the theoretical work has been addressed to characterize the lowest minimum energy crossing point (MECP).[27] Furthermore, for a system of large molecular size as that here considered, the realistic goal is to find the region of coordinates where the MECP could be characterized.

Just to mention two paradigmatic examples, the photostability of the DNA bases[28−31] and the primary photochemical event of visual transduction of the retinal protonated Schiff base[32] are both controlled by the presence of CIs involving the respective hypersurfaces of the ground and lowest electronic excited state. In connection with the present research, it is worth mentioning that recent computational evidence supports that the ultrafast photoinitiated long-range ET in cyclophane-bridged zincporphyrin−quinone complexes is facilitated via a CI.[16,17] The current work represents, however, the first high-level ab initio research of *intermolecular* ET involving *neutral/reduced* species on realistic models related to the photosynthetic RCs. For this purpose, and in order to make the computation manageable, the study has been focused on the following reaction

$$FBC^- + Q \rightarrow FBC + Q^-$$

where FBC/FBC^- represent the neutral/reduced forms of free base chlorin and Q/Q^- the *p*-benzoquinone molecule and *p*-benzosemiquinone radical anion, respectively. As can be seen from Figure 1, the relationship of FBC with Pheo (or BPheo) and Q with the actual primary photosynthetic stable quinone acceptors is clear. Therefore, it is not surprising that FBC and Pheo have similar optical spectra.[10] Substituents in Pheo are most probably used to anchor the chromophores and are expected to play a secondary role for the efficiency of the ET process. The FBC system has been preferred with respect to Pheo (with no symmetry elements), also because the former has somewhat higher molecular symmetry, which represents a noticeable computational advantage without detriment of the conclusions achieved.

To describe properly the electron attachment in FBC and Q, electron correlation has to be included to a large extent.[33−35] It is well-known that anionic systems are more difficult to handle theoretically than neutral molecules.[36] As shown earlier for different molecules, the CASPT2//CASSCF protocol is capable of recovering dynamic electron correlation, yielding accurate electron affinities.[35,37,38] Computation of the $[FBC/Q]^-$ system at the CASPT2 level employing extended basis sets was found to be mandatory in order to lead to conclusive results. Doubtless such calculations have constituted a formidable task, requiring considerable manpower and software/hardware resources. As shall be discussed below, the results reported here give insight on the global conditions and relative donor−acceptor orientation in order to display an efficient ET. In addition, we can safely anticipate that the same principles are expected to control the efficiency of analogous ET-based materials operating under the same basic principles, which might be helpful to bear in mind as guidance for future development on material science.

2. Computational Details

The low-lying excited states of the $[FBC/Q]^-$ system, as well as those of the corresponding isolated moieties, have been studied by using multiconfigurational second-order perturbation theory through the CASPT2 method.[39] The successful performance of the CASPT2 approach in computing spectroscopic properties is well-established.[40−42] State-average CASSCF wave functions were used as zeroth-order wave functions, including in the average procedure the roots of interest. Details about the active spaces and basis sets employed shall be given below as required. To minimize the influence of weakly interacting intruder states at the second-order level, the so-called imaginary level shift technique was employed,[43] being the value of the selected shift 0.2 au. The CASSCF state interaction (CASSI)

TABLE 1: Computed Vertical Electron Affinity (VEA) for Free Base Chlorin (FBC) Employing Different One-Electron Basis Sets[a]

basis set	CASSCF (eV)	CASPT2 (eV)
6-31G	−0.13	0.13
6-31G*	−0.17	0.42
ANO-S[b] C,N[3s2p1d]/H[2s]	0.25	1.05

[a] The active space comprises four MOs (Gouterman's model) with four (five) active electrons for the neutral (anionic) molecule. [b] Primitive sets: C,N (10s6p3d)/H(7s), ref 48.

method[44,45] was used to calculate the transition dipole moments. In the expression for the oscillator strength, the CASSCF transition moment and the energy difference obtained in the CASPT2 computation were employed.

The ground-state geometry for FBC was optimized at the B3PW91/6-31G* level, which has been successfully employed earlier for molecules with similar structure.[46] Geometry optimization was performed within the constraints of the C_{2v} and C_s point groups. The present results are in accordance with previous findings obtained at a comparable level of theory and consistent with the corresponding optimized MP2 structure.[47] On the basis of a previous experience on *p*-benzoquinone,[34] the ground-state geometry of the system (D_{2h} symmetry) was optimized at the π-CASSCF level by including in the active space the π valence orbitals, that is, a total of eight electrons were distributed among the eight π molecular orbitals (MOs). The ANO-S basis set was used with the contraction scheme C,O[3s2p1d]/H[2s].[48] For detailed information about the geometric parameters, the reader is referred to the Supporting Information.

The calculations were performed with the tools available in the MOLCAS-6[49] and the Gaussian 98[50] quantum chemistry packages.

3. Results and Discussion

3.1. Calibration Calculations: Electron Affinities. The vertical electron affinity (VEA) of FBC was calculated using the CASSCF and CASPT2 methods. The influence of the results upon increasing the flexibility of the basis sets was carefully analyzed. The active space comprised four molecular orbitals, which correspond to the Gouterman's model.[51−53] Accordingly, four and five electrons were used as active for the neutral and anion, respectively. As can be seen in Table 1, the computed VEA depends on both the level of calculation and the type of basis set employed. Only with the larger ANO-type basis set the VEA becomes positive at the CASSCF level. In order words, as reflected by the negative values (6-31G and 6-31G* results), the FBC anion is predicted to be unbound with respect to electron attachment at the CASSCF level of theory. When dynamic electron correlation is included by using the CASPT2 method, positive VEA are obtained with the three basis sets employed, increasing from 0.13 to 1.05 eV upon enlargement of the basis set. On the other hand, the difference between the CASPT2 and CASSCF results calculated with the ANO-S basis sets is 0.8 eV, which is entirely due to the inclusion of dynamic electron correlation through the CASPT2 approach. Quite impressive, indeed, considering it is just a second-order method, although it is not surprising on the basis of previous experience.[37,54] Therefore, our best estimate for the VEA of FBC is 1.05 eV. Because of the single configurational nature of the CASSCF wave functions of both the neutral and radical anion systems and taking into consideration the inherent flexibility of the ANO-type contraction employed, the result can be considered to be in practice converged (±0.1 eV) with respect to further improvements (enlargement of the active space and basis set). The VEA of FBC is expected to be a well-defined positive value in view of the important role that this molecule has in biological processes and the known redox potential.[10] As far as we know, there is lack of experimental datum to compare with. Nevertheless, the computed VEA of FBC (1.05 eV) is comparable to that obtained at the IP-EOM-CC level for free base porphin (1.07 eV)[55] employing a basis set of similar quality.

The relevant contribution of dynamic electron correlation (CASSCF vs CASPT2 results) on the computed EA of *p*-benzoquinone has been discussed elsewhere.[35] Employing the ANO-S C,O[3s2p1d]/H[2s] basis set, the VEA for *p*-benzoquinone is here computed to be 1.63 eV at the π-CASPT2 level, which is consistent with earlier findings.[34,35] A previous determination at the same level of theory yielded 1.64 eV using a larger basis set, in particular the ANO-L C,O[4s3p1d]/H[2s1p] + 1s1p1d diffuse functions. Therefore, at least for the low-lying states, the ANO-S C,O[3s2p1d]/H[2s] basis set is flexible enough for the treatment of *p*-benzoquinone in $[FBC/Q]^-$. Furthermore, in accordance with the single configurational nature of the neutral ground state and the *p*-benzosemiquinone radical anion, the calculated VEA at the restricted open-shell MP2 level employing the ANO-S C,O[3s2p1d]/H[2s] basis set, 1.77 eV, is also of comparable quality, just 0.14 eV above the π-CASPT2 result, giving insight into the (minimum) active space required for the treatment of the $[FBC/Q]^-$ system. Therefore, it is expected that the ANO-S type basis set with the contraction C,N[3s2p1d]/H[2s] and the active space of five electrons distributed in five molecular orbitals will be able to describe accurately the ET involved in $[FBC/Q]^-$.

3.2. Electron-Transfer Between Free Base Chlorin Radical Anion and Quinone. Potential energy curves (PECs) for two different oxidation states of the system $[FBC/Q]^-$ along the intermolecular distance *R* have been built for three different parallel arrangements, with the subsystems kept fixed at the respective ground-state equilibrium geometry. As shown in Figure 2, the orientations considered are defined by the angle θ formed between the binary symmetry axis C_2 of FBC (perpendicular to the axis containing the inner pyrrolic hydrogen atoms) and the axis passing through the oxygen atoms of the Q molecule. The results obtained at the CASPT2 level are depicted in Figure 2. The ANO-S C,N,O[3s2p1d]/H[2s] basis set was employed throughout. In $[FBC/Q]^-$, as derived from calibration calculations on FBC and Q, the active space for the reference CASSCF wave function comprised five MOs (four of FBC and one of Q) and five active electrons. At each intermolecular distance recorded in the pictures, state-average CASSCF calculations of the lowest three roots were carried out for the global system at $\theta = 0°$ (C_s symmetry) and $\theta = 45°$ (C_1 symmetry), whereas two roots of each symmetry were computed for the C_s $\theta = 90°$ orientation. Since the third root is not relevant for the ET process here considered, it will not be further discussed. The CASSCF results have been collected in the Supporting Information.

Our study starts once the photoinduced charge separation has occurred in the photosynthetic RCs and the $Pheo^-$ species (or $BPheo^-$) has been consequently produced. Thus, one should be placed in the right-hand side of the PECs of Figure 2. Of course, at infinity separation (here computed as two independent fragments) the three asymptotic limits, corresponding to the three different orientations, become equivalent and equal to the (FBC^- + Q), which is about 0.7 eV above the lowest limit (FBC +

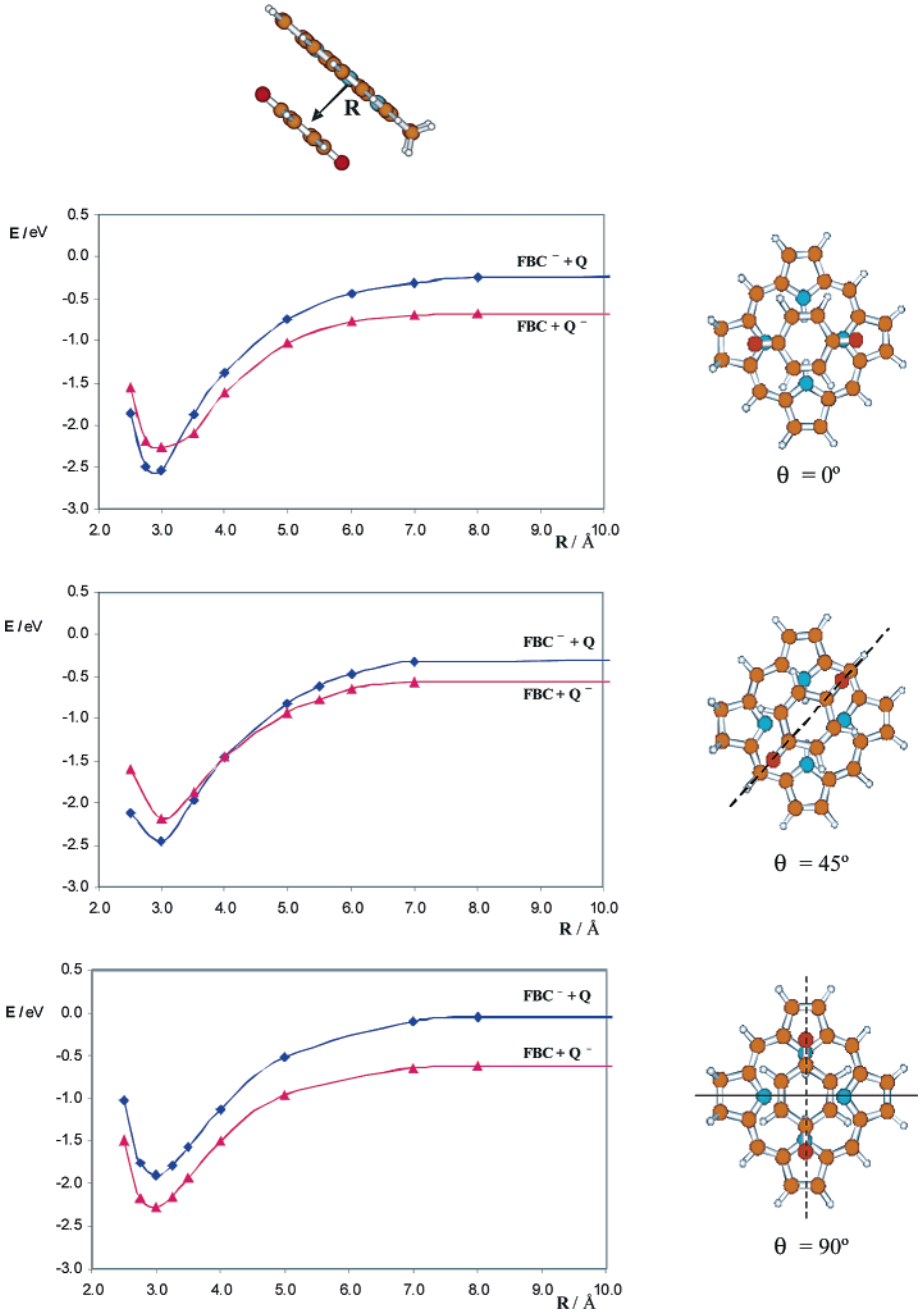

Figure 2. CASPT2 potential energy curves for the $[FBC/Q]^-$ system built with respect to the intermolecular distance *R*. The three different orientations are defined by angle θ (see the text).

Q^-). That energy difference is precisely the energy difference of the VEAs computed for Q and FBC. It is worth noting that the reactants of interest, ($FBC^- + Q$), correspond at large *R* to the lowest excited state of the $[FBC/Q]^-$ system. Since the Q molecule has a higher VEA than FBC, the noninteracting FBC plus Q^- system becomes the ground state at large *R*.

As can be readily seen from Figure 2, the energy separation between the two states at $R = 10$ Å is the largest for the orientation at $\theta = 90°$ and the smallest at $\theta = 45°$, between them being the situation at $\theta = 0°$. In order words, that at $R = 10$ Å ($\theta = 90°$) the energy difference between the two states is already close to the asymptotic limit at infinity reveals that the interaction between FBC^- and Q is not as strong as compared to the other arrangements. Since the CASSCF wave functions of $FBC^-$and Q^- are basically described by a single configuration with the extra electron located in the LUMO-like natural orbital, structures that facilitate the overlap between the two LUMOs lead to a more pronounced interaction and the occurrence of the state-crossing. According to the topology of the LUMOs of FBC and Q (see Figure 3), the overlap between those decreases at $\theta = 90°$. Consequently, there is no crossing between the two PECs for $\theta = 90°$ (see Figure 2, bottom). A similar situation can be expected for perpendicular and other intermediate molecular arrangements; therefore, they were not taken into consideration.

On the contrary, the PECs do intersect at the other two orientations. The most effective interaction occurs at $\theta = 45°$, which hints to a larger overlap between the respective LUMOs. For this reason, when the two moieties get progressively closer, the crossing between the two curves appears earlier at $\theta = 45°$, at about 4 Å, with respect to $\theta = 0°$, at about 3.3 Å, reflecting in the latter a somewhat less efficient interaction. Therefore, it is expected that the ET process becomes most efficient at $\theta = 45°$, associated with a relatively higher rate constant.[19] The

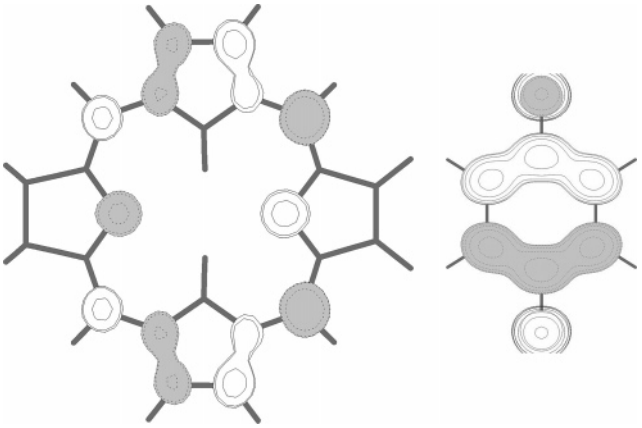

Figure 3. LUMOs of FBC (left) and Q (right).

actual crossing point should hopefully correspond to a CI and its geometry most probably should display for the FBC skeleton a distortion from planarity. This suggestion is inspired by the well-known effects that nonplanarity causes on the lifetimes of singlet excited states in porphyrin derivatives[8] and DNA nucleobases.[28−31] The lifetimes can be considerably shortened (from nanoseconds to picoseconds) in nonplanar chromophores because of the presence of many different decay paths and funnels connecting the excited and ground states.[30,31,56] Corroboration of this hypothesis represents by itself a formidable objective and should be addressed in the future with the necessary expected software and hardware improvements. We can just remark at present that such crossings do exist in regions where the degeneracy of electronic states is found in multidimensional systems,[56] reinforcing previous suggestions by Dreuw et al.[17] on the important role that crossing seams play in the ultrafast ET processes occurring ubiquitously in many biochemical systems of current interest. Curves in Figure 2 should not be seen, however, as a representation of the ultrafast ET mechanism in RC but demonstrate that the involvement of CIs in the ET process is possible for certain donor−acceptor orientations.

At $\theta = 45°$ the minima $(FBC^- + Q)_{min}$ and $(FBC + Q^-)_{min}$ are found at about $R = 3$ Å. The latter is placed vertically about 0.3 eV above the former, with a computed oscillator strength for the related transition of 0.03. It is worth mentioning that the basis set superposition error (BSSE) computed using the counterpoise procedure[57] was shown not to affect the vertical relative energies at given intermolecular distances, because the magnitude of the correction is the same for both states. At short intermolecular distances the $FBC^- + Q$ system becomes the ground state, which is connected adiabatically to $FBC + Q^-$ at infinity. Depending on the topology of the actual CI, both minima may be populated. Ideally, such topology should be favoring population of the charge-transfer state $(FBC + Q^-)$. A number of crossing and recrossings probably occur around the CI region leading to the fulfillment of ET. By a subsequent increase of the intermolecular distance the products of the ET reaction, neutral FBC and reduced quinone Q^-, are ultimately collected. The primary reduced quinone is so ready to transfer an electron to the secondary quinone and Pheo (FBC in our model) is willing to be involved again in new photoinduced charge-transfer process in the RCs.

4. Conclusions

Delineation of the mechanism of electron transfer from a reduced pheophytin-like system to a quinone-like molecule, with special emphasis on the role of the quinone movement during the process, has been the major aim of the present research. Because of the inherent difficulties in the theoretical determination of electron affinities, high-level ab initio methodologies, CASSCF and CASPT2, have been applied. As far as we know, it is the first time that this kind of research has been undertaken. Therefore, the present findings can be used as reference results to be compared to less demanding theoretical approaches that could undertake, however, models of larger molecular size.

In summary, we conclude that intermolecular ET between a reduced (charged) donor and an acceptor can be formulated as a dance of three steps. First, both systems have to get close enough, with the right relative orientation, to allow overlap between the singly occupied MO of the donor and the LUMO of the acceptor. Second, a number of state-crossings related to multiple conical intersections may then take place, resembling the common procedure of internal conversion controlled by crossing seams, as is normally recognized in modern nonadiabatic photochemistry. Third, a subsequent separation of the produced moieties leads to the products: neutral donor and reduced acceptor.

A vast amount the work involving synthesis of biomimetic materials for artificial photosynthesis deals with molecules made of covalently linked subunits. According to the present results, noncovalently π-staked materials should also operate efficiently. It is not surprising, since they are used by nature.

Acknowledgment. The research reported has been supported by the MEC-FEDER project CTQ2004-01739 and by project GV06-192 of the Generalitat Valenciana. G.O.G. gratefully acknowledges a Ph.D. (FPU) fellowship from the Spanish MEC.

Supporting Information Available: Cartesian coordinates for the optimized structures and CASSCF profiles (PDF). This material is available free of charge via the Internet at http://pubs.acs.org.

References and Notes

(1) Allen, J. P.; Williams, J. C. *FEBS Lett.* **1998**, *438*, 5.
(2) Govindjee; Foyer, C. H. *Photosynth. Res.* **2005**, *85*, 251.
(3) Whitmarsh, J.; Govindjee. In *Concepts in Photobiology: Photosynthesis and Photomorphogenesis*; Singhal, G. S., Renger, G., Irrgang, K. D., Sopory, S., Govdinjee, Eds.; Kluwer: Pittsburgh, 1999.
(4) Dekker, J. P.; van Grondelle, R. *Photosynth. Res.* **2000**, *63*, 195.
(5) Zouni, A.; Witt, H. T.; Kern, J.; Fromme, P.; Krauss, N.; Saenger, W.; Orth, P. *Nature* **2001**, *409*, 739.
(6) McDonald, M. S. *Photobioloogy of higher plants*; John Wiley & Sons: Chichester, UK, 2003.
(7) Ferreira, K. N.; Iverson, T. M.; Maghlaoui, K.; Barber, J.; Iwata, S. *Science* **2004**, *303*, 1831.
(8) Fajer, J. *Photosynth. Res.* **2004**, *80*, 165.
(9) Levanon, H.; Möbius, K. *Annu. Rev. Biophys. Biomol. Strut.* **1997**, *26*, 495.
(10) Hasegawa, J.; Ozeki, Y.; Ohkawa, K.; Hada, M.; Nakatsuji, H. *J. Phys. Chem. B* **1998**, *102*, 1320.
(11) Blomberg, M. R. A.; Siegbahn, P. E. M.; Babcock, G. T. *J. Am. Chem. Soc.* **1998**, *120*, 8812.
(12) Siegbahn, P. E. M.; Crabtree, R. H. *J. Am. Chem. Soc.* **1999**, *121*, 117.
(13) Sundholm, D. *Chem. Phys. Lett.* **1999**, *302*, 480.
(14) Parusel, A. B. J.; Grimme, S. *J. Phys. Chem. B* **2000**, *104*, 5395.
(15) Sundström, V. *Prog. Quantum Electron.* **2000**, *24*, 187.
(16) Worth, G. A.; Cederbaum, L. S. *Chem. Phys. Lett.* **2001**, *338*, 219.
(17) Dreuw, A.; Worth, G. A.; Cederbaum, L. S.; Head-Gordon, M. *J. Phys. Chem. B* **2004**, *108*. 19049.
(18) Siegbahn, P. E. M.; Blomberg, M. R. A. *Biochim. Biophys. Acta* **2004**, *1655*, 45.
(19) Barbara, P. F.; Meyer T. J.; Ratner A. M. *J. Phys. Chem.* **1996**, *100*, 13148.
(20) Marcus, R. A. *Annu. Rev. Phys. Chem.* **1964**, *15*, 155.
(21) Blancafort, L.; Jolibois, F.; Olivucci, M.; Robb, M. A. *J. Am. Chem. Soc.* **2001**, *123*, 722.

(22) *Conical Intersections: Electronic Structure, Dynamics and Spectroscopy*; Domcke, W., Yarkony, D. R., Köppel, H., Eds.; World Scientific: Singapore, 2004.
(23) Computational Photochemistry. In *Theoretical and Computational Chemistry*; Olivucci, M., Ed.; Elsevier Publishing: Amsterdam, 2005; Vol. 16.
(24) Fernández, E.; Blancafort, L.; Olivucci, M.; Robb, M. A. *J. Am. Chem. Soc.* **2000**, *122*, 7528.
(25) Jolibois, F.; Bearpark, M. J.; Klein, S.; Olivucci, M.; Robb, M. A. *J. Am. Chem. Soc.* **2000**, *122*, 5801.
(26) Sinicropi, A.; Pischel, U.; Basosi, R.; Nau, W. M.; Olivucci, M. *Angew. Chem., Int. Ed.* **2000**, *39*, 4582.
(27) Serrano-Andrés, L.; Merchán, M.; Lindh, R. *J. Chem. Phys.* **2005**, *122*, 104107.
(28) Merchán, M.; Serrano-Andrés, L. *J. Am. Chem. Soc.* **2003**, *125*, 8108.
(29) Merchán, M.; Serrano-Andrés, L.; Robb, M. A.; Blancafort, L. *J. Am. Chem. Soc.* **2005**, *127*, 1820.
(30) Serrano-Andrés, L.; Merchán, M.; Borin, A. C. *Proc. Natl. Acad. Sci. U.S.A.* **2006**, *103*, 8691.
(31) Serrano-Andrés, L.; Merchán, M.; Borin, A. C. *Chem.—Eur. J.* **2006**, *12*, 6559.
(32) González-Luque, R.; Garavelli, M.; Bernardi, F.; Merchán, M.; Robb, M. A.; Olivucci, M. *Proc. Natl. Acad. Sci. U.S.A.* **2000**, *97*, 9379.
(33) Serrano-Andrés, L.; Merchán, M.; Rubio, M.; Roos, B. O. *Chem. Phys. Lett.* **1998**, *295*, 195.
(34) Pou-Amérigo, R.; Merchán, M.; Ortí, E. *J. Chem. Phys.* **1999**, *110*, 9536.
(35) Pou-Amérigo, R.; Serrano- Andrés, L.; Merchán, M.; Ortí, E.; Forsberg, N. *J. Am. Chem. Soc.* **2000**, *122*, 6067.
(36) Serrano-Andrés, L.; Merchán, M. In *Encyclopedia of Computational Chemistry*; Schleyer, P. (v) R., et al., Eds.; Wiley: Chichester, UK, 2004.
(37) Frutos, L. M.; Castaño, O.; Merchán, M. *J. Phys. Chem. A* **2003**, *107*, 5472.
(38) Rubio, M.; Merchán, M.; Ortí, E.; Roos, B. O. *J. Phys. Chem.* **1995**, *99*, 14980.
(39) Andersson, K.; Malmqvist, P.-Å.; Roos, B. O. *J. Chem. Phys.* **1992**, *96*, 1218.
(40) Roos, B. O.; Fülscher, M. P.; Malmqvist, P.-Å; Serrano-Andrés, L.; Pierloot, K.; Merchán, M. *Adv. Chem. Phys.* **1996**, *93*, 219.
(41) Merchán, M.; Serrano-Andrés, L.; Fülscher, M. P.; Roos, B. O. In *Recent Advances in Multireference Methods*; Hirao, K., Ed.; World Scientific Publishing: Singapore, 1999.
(42) Serrano-Andrés, L.; Merchán, M. *J. Mol. Struct. THEOCHEM* **2005**, *729*, 99.
(43) Forsberg, J.; Malmqvist, P.-Å. *Chem. Phys. Lett.* **1997**, *274*, 196.
(44) Malmqvist, P.-Å. *Int. J. Quantum Chem.* **1986**, *30*, 479.
(45) Malmqvist, P.-Å.; Roos, B. O. *Chem. Phys. Lett.* **1989**, *155*, 189.
(46) Rubio, M.; Roos, B. O.; Serrano-Andrés, L.; Merchán, M. *J. Chem. Phys.* **1999**, *110*, 7202.
(47) Almöf, J.; Fischer, T. H.; Gassman, P. G.; Ghosh, A.; Häser, M. *J. Phys. Chem.* **1993**, *97*, 10964.
(48) Pierloot, K.; Dumez, B.; Widmark, P.-O.; Roos, B. O. *Theor. Chim. Acta* **1995**, *90*, 87.
(49) Andersson, K.; Barysz, M.; Bernhardsson, A.; Blomberg, M. R. A.; Carissan, Y.; Cooper, D. L.; Cossi, M.; Fülscher, M. P.; Gagliardi, L.; de Graaf, C.; Hess, B.; Hagberg, G.; Karlström, G.; Lindh, R.; Malmqvist, P.-Å.; Nakajima, T.; Neogrády, P.; Olsen, J.; Raab, J.; Roos, B. O.; Ryde, U.; Schimmelpfennig, B.; Schütz, M.; Seijo, L.; Serrano-Andrés, L.; Siegbahn, P. E. M.; Stålring, J.; Thorsteinsson, T.; Veryazov, V.; Widmark, P.-O. *MOLCAS*, version 6.0; Department of Theoretical Chemistry, Chemical Centre, University of Lund: Lund, Sweden, 2004.
(50) Frisch, M. J.; Trucks, G. W.; Schlegel, H. B.; Scuseria, G. E.; Robb, M. A.; Cheeseman, J. R.; Zakrzewski, V. G.; Montgomery, J. A., Jr.; Stratmann, R. E.; Burant, J. C.; Dapprich, S.; Millam, J. M.; Daniels, A. D.; Kudin, K. N.; Strain, M. C.; Farkas, O.; Tomasi, J.; Barone, V.; Cossi, M.; Cammi, R.; Mennucci, B.; Pomelli, C.; Adamo, C.; Clifford, S.; Ochterski, J.; Petersson, G. A.; Ayala, P. Y.; Cui, Q.; Morokuma, K.; Malick, D. K.; Rabuck, A. D.; Raghavachari, K.; Foresman, J. B.; Cioslowski, J.; Ortiz, J. V.; Stefanov, B. B.; Liu, G.; Liashenko, A.; Piskorz, P.; Komaromi, I.; Gomperts, R.; Martin, R. L.; Fox, D. J.; Keith, T.; Al-Laham, M. A.; Peng, C. Y.; Nanayakkara, A.; González, C.; Challacombe, M.; Gill, P. M. W.; Johnson, B.; Chen, W.; Wong, M. W.; Andrés, J. L.; Head-Gordon, M.; Replogle, E. S.; Pople, J. A. *Gaussian 98*, revision A.6; Gaussian, Inc.: Pittsburgh, 1998.
(51) Gouterman, M. *J. Chem. Phys.* **1959**, *30*, 1139.
(52) Gouterman, M.; Wagnière, G.; Snyder, L. C.; *J. Mol. Spectrosc.* **1963**, *11*, 108.
(53) Weiss, C.; Kobayashi, H.; Gouterman, M. *J. Mol. Spectrosc.* **1965**, *16*, 415.
(54) Garavelli, M.; Bernardi, F.; Cembran, A.; Castaño, O.; Frutos, L. M.; Merchán, M.; Olivucci, M. *J. Am. Chem. Soc.* **2002**, *124*, 13770.
(55) Gwaltney, S. R.; Bartlett, R. J. *J. Chem. Phys.* **1998**, *108*, 6790.
(56) Truhlar, D. G.; Mead, C. A. *Phys. Rev. A* **2003**, *68*, 032501.
(57) Boys, S. F.; Bernardi, F. *Mol. Phys.* **2002**, *100*, 65.